Heat and mass transfer to/from active particles in a fluidized bed - An analysis of the Baskakov-Palchonok correlation

International Journal of Heat and Mass Transfer 168 (2021) 120860

Contents lists available at ScienceDirect

International Journal of Heat and Mass Transfer

journal homepage: www.elsevier.com/locate/hmt

Heat and mass transfer to/from active particles in a fluidized bed—An analysis of the Baskakov-Palchonok correlation

Bo Leckner

Division of Energy Technology, Chalmers University of Technology, 41296 Göteborg, Sweden

ARTICLE INFO

Article history:
Received 2 October 2020
Revised 2 December 2020
Accepted 20 December 2020

Keywords:
Heat transfer
Mass transfer
Particles
Active particles
Fluidized bed
Correlation

ABSTRACT

Heat and mass transfer to or from single active particles surrounded by inert (passive) particles in a fluidized bed has been investigated based on published correlations. Special emphasis is on the application of a proposal by Baskakov, further developed by Palchonok. This representation describes heat and mass transfer as a function of the size ratio of inert to active particles. Two limits have been chosen: the limit of small active particles, where the active and the inert particles are equal, and the limit of large active particles, where the influence of the size of the active particle has vanished. The presentation aims at finding a suitable relationship, describing the size ratio of inert to active particles on heat and mass transfer to/from particles in fluidized beds and to critically evaluate its usefulness. It seems that the agreement between available correlations is qualitative and only approximate estimations can be made. A generalized scheme for calculations is presented. The formulation is made for bubbling fluidization. A discussion is presented on its use in circulating fluidized bed applications for fuel conversion as well.

1. Introduction

Heat and mass transfer to or from active particles surrounded by inert (passive) particles in a fluidized bed has many applications, of which conversion of solid fuel (devolatilization, combustion or gasification) is an important one. This topic has been treated frequently in the literature, and many correlations for the determination of heat and mass transfer coefficients have been proposed, often starting from single-phase expressions. Judging from recent (last decades) literature on conversion of fuels, there is no consensus on which representation to use, especially not for heat transfer. The procedure proposed by Baskakov et al. [1] and subsequently elaborated by Palchonok [2,3], is just one of several alternatives, but it has not been sufficiently well documented and analysed. This is the purpose of the present work. The heat transfer concerns small particles, where minimum fluidization velocity (u_{mf}) plays a role, and large particles, where a maximum heat transfer occurs at an optimum fluidization velocity. For mass transfer, no significant influence of the fluidization velocity u has been observed for superficial velocities above the minimum one u_{mf}, see for example [4]. Recently, a Baskakov-Palchonok model of heat transfer was mentioned in a study by von Berg et al. [5] on the influence of the fluidization velocity. The information was taken from an overview on gasification modelling [6], where only a brief survey was given on Palchonok's model formulation. This is another reason to explain the background and the validity of the concept more extensively.

The comparison with independent data is made by selecting a few model-free correlations to check the consistency of the formulation studied. A comprehensive overview on heat and mass transfer to particles is found in Di Natale et al. [7], which can be referred to for a more complete picture. The only remark that should be done here is that, because of a misinterpretation, the work of Palchonok got an unfavourable evaluation by Di Natale et al. Furthermore, the present topic area, fluidized beds of inactive bed particles containing a minor quantity of active particles whose size may differ from that of the inactive bed particles, the much-quoted work of Gunn [8] is not included in the present survey.

The transfer mechanisms are gas conduction and gas and particle convection (radiation can be added but is not treated here). The well-known correlations for heat and mass transfer to particles in single-phase flow [9,10] express the mechanisms of gas conduction and convection based on the analogy of heat and mass transfer. In the fluidized bed application, there is an additional mechanism in the case of heat transfer, particle convection, which breaks the analogy. However, the analogy is still useful for the gas-convective component, as will be explained below. Because of the impact of bed particles in a fluidized bed, another influencing pa-

E-mail address: ble@chalmers.se

https://doi.org/10.1016/j.ijheatmasstransfer.2020.120860

Nomenclature

$Ar=d_i^3 g\rho_g(\rho_s-\rho_g)/\mu^2$	Archimedes number
c_p	specific heat, J/kg,K
d	diameter, m or mm
D	diffusivity, m^2/s
f()	function, -
g	gravity, m/s^2
h	heat transfer coefficient, W/m^2K
H	height of combustion chamber, m
j	mass transfer factor, -
k	thermal conductivity, W/ms
Nu=hd/k	Nusselt number, -
P	pressure, Pa
$Pr=\mu c_p/k$	Prandtl number, -
$Re=ud/\nu$	Reynolds number, -
$Sh=\beta d/D$	Sherwood number, -
$Sc=\nu/D$	Schmidt number, -
T	temperature, K
u	velocity, m/s
β	mass transfer coefficient, m/s
δ	void phase, -
ε	voidage, -
ν	kinematic viscosity, m^2/s
μ	dynamic viscosity, kg/ms
ρ	density, kg/m^3

Subscripts, superscripts

a	active particle
e	emulsion phase
g	gas
i	inert particle, bed particle
mf	minimum fluidization condition
m	superscript in Prins' correlation, coefficient
n	decay coefficient, coefficient
s	solisds, particle, slip
1∞	large active particle

rameter plays a role, namely the ratio of the sizes of active (d_a) and inactive (d_i) particles.

2. The Baskakov-Palchonok model

Available data on heat and mass transfer in fluidized bed can be expressed as *Nu(Sh) = f(Ar, Pr (Sc),d_i/d_a),* where the size of an active particle is contained between a small-particle limit and a large active particle limit. As a small-particle limit, with equally sized active (d_a) and bed particles (d_i) is chosen (index 1), established by a comparison with available data, Palchonok [2,3], without considering particle densities, as they were shown to only have a minor impact as long as the particles are well fluidized,

$$Nu_1 = \frac{2}{\left(1-\left(1-\varepsilon_{mf}\right)^{1/3}\right)} + 0.117 Ar_i^{0.39} Pr^{0.33} \tag{1}$$

$$Sh_1 = 2\varepsilon_{mf} + 0.117 Ar_i^{0.39} Sc^{0.33} \tag{2}$$

For large active objects, the size of the object ceases to be important, and results from heat and mass transfer measurements to large objects in fluidized beds can be used as a basis for the large active-particle limit $d_a >> d_i$. Such data were measured for fixed, rounded objects of a size between 10 and 60 mm in a fluidized bed at 1170 K, Baskakov et al. [1,11].

$$Nu_{i,\infty} = 0.85 Ar_i^{0.19} + 0.006 Ar_i^{0.5} \,\mathrm{Pr}^{0.33} \tag{3}$$

$$Sh_{i,\infty} = 0.009 Ar_i^{0.5} Sc^{0.33} \tag{4}$$

The gas convective component (Eq. (4) and the second term of Eq. (3)) was obtained from naphthalene samples, 11–50 mm in diameter and 70–132 mm long, inserted vertically in well fluidized beds at 330 K. Conduction $2\varepsilon_{mf}(d_i/d_a)$ could be added to Eq. (4), but the term is very small (d_a large), and it is only used for completeness when plotting over a wide range of *Ar*.

The active particles of a size d_a exchange heat or mass with the gas and the surrounding inert particles whose size is d_i. This can be described by interpolation between the small and large particle limits, expressed to obtain the desired Nusselt and Sherwood numbers Nu_i and Sh_i

$$(Nu_i - Nu_{i,\infty})/(Nu_1 - Nu_{i,\infty}) = f(d_i/d_a) \tag{5}$$

$$(Sh_i - Sh_{i,\infty})/(Sh_1 - Sh_{i,\infty}) = f(d_i/d_a) \tag{6}$$

The interpolation function *f(),* to be discussed below, is determined by fitting to various measured data sets and correlations. Preferably model-free correlations are looked for.

Eqs. (1)–(6) are related to the inert particle size d_i, but the results are normally desired related to the active particle size d_a. Transformations are carried out as follows:

$$Nu_a = Nu_i d_a/d_i$$
$$\text{with} Nu_i = Nu_{i,\infty} + (Nu_1 - Nu_{i,\infty}) f(d_a/d_i) \text{from Eq.(5)} \tag{7}$$

$$Sh_a = Sh_i d_a/d_i$$
$$\text{with} Sh_i = Sh_{i,\infty} + (Sh_1 - Sh_{i,\infty}) f(d_a/d_i) \text{from Eq.(6)} \tag{8}$$

Below, the small and large particle limits will be defined.

2.1. The small active particle limit

Nusselt and Sherwood numbers for the $d_a = d_i$ limit were reported by Palchonok et al. [2], referring to a number of measured data sets and models. A few of those plus some more recent data are presented in Fig. 1 and Table 1, showing that the agreement is quite good. The data employed are valid for the condition of $d_a = d_i$.

The first term on the right-hand side of Eqs. (1) and (2) is the conduction term inherited from the derivation of the single-phase expressions [9]. For the case of $d_i = d_a$ in a fluidized bed, this term considers heat or mass conducted through the gas to an active particle, which is not exposed to a convective movement of the gas. Then, a heat balance on the particle becomes

$$h\pi d_a^2 (T_a - T_i) = \frac{2\pi k_g (T_a - T_i)}{1/d_a - 1/d_e} \tag{9}$$

where h (W/m^2,K) is the heat transfer coefficient, k_g (W/m,K) the thermal conductivity of the gas, T_a and T_i (K) are the temperatures of the active particle d_a and of the surrounding inert particles. Integration from the surface of the particle to the end of the boundary layer d_e, going to infinity, yields the well-known result for a single-phase situation: $Nu = Sh = 2$ (see Eq. (10)).

In the case of mass transfer to an active particle surrounded by non-absorbing inert particles, the concentration boundary layer still extends itself, but the transfer is shielded by the surrounding inert particles, impeding the transfer of gas, and $Sh_a = \varepsilon 2$ was suggested [16] where ε is the voidage of the surrounding medium. In the case of heat transfer, the surrounding inert particles absorb heat and limit the extension of the boundary layer d_e. From Eq. (9) we have

$$Nu_a = \frac{2}{(1 - d_a/d_e)} \tag{10}$$

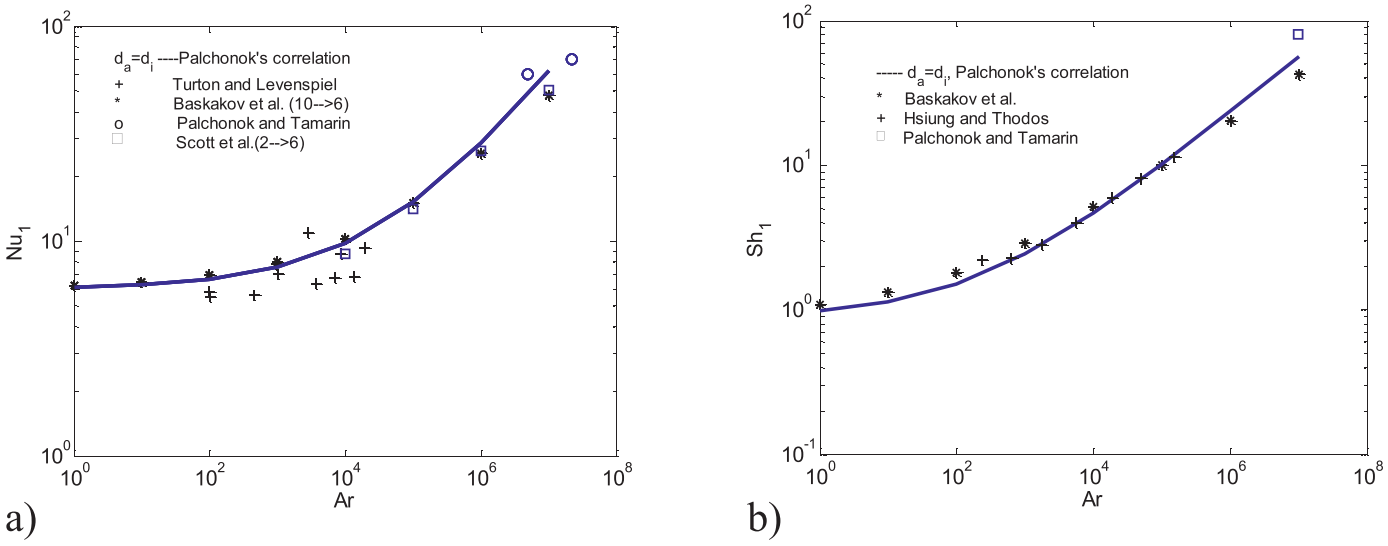

Fig. 1. The $d_a = d_i$ limit. Palchonok's correlation (Eqs. (1) Fig. 1a) and ((2) (Fig. 1b)) is derived from various sets of measurement data from freely moving particles of the same size as the bed material, evaluated at 300 K. See also [2].

Table 1
Correlations for equal particle sizes d_a=d_i.

Reference	Correlation	Experimental conditions
Turton et al. [12]	$Nu = 0.46(\mathrm{Re}/\varepsilon)_{mf}^{0.09}[\frac{(1-\varepsilon_{mf})\rho_s c_{p,s}}{\varepsilon_{mf}\rho_g c_{p,g}}]^{0.36}$	$0.106<d_i<0.670$; d_a wires; $920<\rho_s<2700$, $300<T<450$ K
Palchonok and Tamarin [13]	$Nu = 0.41Ar^{0.3}$	$1.55\bullet10^5<Ar<2.2\bullet10^7$ $900<\rho_s<2500$; T=300 K
Hsiung and Thodos [14]	$\frac{Sh}{\mathrm{Re}_{mf}\cdot Sc^{0.33}} = 0.040 + \frac{2.12}{\mathrm{Re}_{mf}^{0.59}} + \frac{0.62}{\mathrm{Re}_{mf}^{1.31}}$	Seven d_i between 0.248 and 2.0 mm. 300-350 K
Baskakov et al. [11]	$\mathrm{Sh_i}=1+0.26(\mathrm{ArSc})^{0.33}$	$0<Ar<10^8$. Temperature not given, probably 300 K
Scott et al. [15]	See Table 2	

An active particle is in a particle phase, where it is surrounded by inert particles. The packing is not necessarily regular, but for modelling purposes it was assumed to be cubical with a voidage of $\varepsilon = 0.48$. The equivalent boundary layer, extending from d_a to d_e, is obtained from the space defined by $\pi d_a^3/6/(\pi d_e^3/6) = (1-\varepsilon)$. With $d_a/d_e=(1-\varepsilon)^{1/3}$, Eq. (10) yields $Nu_a\approx10$ as used by Baskakov et al. [1] and also proposed by Zabrodsky [17]. Palchonok et al. [2] included the surrounding gas space $d_a^3 - \pi d_a^3/6$ and added also the gas lenses formed by the 6 adjacent spheres in the cubical packing, $6(\pi d_a^3/24)$, calculated as a difference in volume between a cylinder and the half-sphere of the adjacent particle. Then, they arrived at $Nu_a \approx 6$.

Obviously, these results are approximate, and further, the condition of low velocity contradicts fluidization, which does not allow velocities lower than that of minimum fluidization. However, the estimation serves the purpose of providing a point for extrapolation of the results in the low-velocity range, and, in fact, the deviation is similar to that in single-phase flow at increasing gas velocity [9], when the convective terms were simply added to the conductive term.

The reason why d_i is taken as a characteristic size of Sh_i and Nu_i Eqs. 7, (8) is that the large active-particle limit is expressed in this way, being independent of the active particle size d_a, but related to the bed particles (d_i).

The second term on the right-hand side (gas convection) in Eqs. (1, 2) was determined by a fit to measurement data, equal for heat and mass transfer. The similarity between the two equations implies that the analogy of heat and mass transfer was valid in this case. When $d_a = d_i$, the active particle is contained in, and moves with, the matrix of inert particles. Then it is reasonable to think that the relative movement between the active and inert particles is insignificant, so there is no contribution from particle convection. Gas convection rules the transfer. Support for this is found in [18], where the heat transfer caused by particle convection tends towards zero in beds of equal active and inert particle sizes, leaving gas conduction and convection as the sole sources of transfer. Another interesting support was given by Palchonok [19] who showed the similarity between a fluidized bed dominated by gas convection and the gas-convective transfer in fixed beds. In beds of large particles, the impact of gas convection was shown in [19], comparing the part of Eq. (1) that was determined by mass transfer (gas convection) with the correlation of Palchonok and Tamarin [13]: at $Ar > 4\bullet10^6$ gas convection was already dominant (see also Fig. 2).

Because of the similarity of heat and mass transfer, the data of Baskakov et al. [11] in Fig. 1 are valid both for heat and mass transfer, which also shows that there is no contribution from particle-convective heat transfer in this fluidization situation where all particles are equally large. In the comparison of Fig. 1, the conductive term of Baskakov et al. (amounting to 10) was replaced by 6 to coincide with Palchonok's value, a reasonable adjustment, considering the derivation of this term. Likewise, 2ε as in Eq. (2) is maintained instead of the simplified form $2\varepsilon \approx 1$ used by Baskakov et al. [11]. Both Hsiung and Thodos [14] and Turton et al. [12] produced well known unique sets of data in this difficult experimental range. Scott et al. [15], owing to their experimental technique, had to pay the prize of using quite large bed particles to attain $d_a = d_i$, and their data are found at high Archimedes numbers.

2.2. The large active particle limit

When the active particle is larger than the surrounding bed particles, it will not readily move along with the bed particles, but it will experience a relative movement with respect to these particles. Gradually, as the active particle increases in size, this movement of the bed particles becomes similar to the classic particle convection heat transfer situation in fluidized beds described by the "packet theory" (see any textbook on fluidization). The gas convection may also be affected by the formation of bubbles around the active particle depending on its degree of mobility. There are two aspects: one concerns the influence of the size of the active particle, and the other the difference in heat or mass transfer between a fixed and a mobile active particle. Equations (3) and (4) were introduced as limiting cases when the size of the active particle no longer plays a role, and only the size of the bed particles and property data are important.

The gas convective component in Eqs. (3) and (4) was determined from mass transfer measurements [20, 1] and was applied also for heat transfer according to the analogy of heat and mass transfer. The relationships were obtained by fitting to various data as described in [1]. The small difference between the terms for heat and mass transfer in Eqs. (3) and (4) most likely originates from such fits to data made at different occasions.

Fig. 2 illustrates the contributions corresponding to particle and gas convective heat transfer to a large active particle surrounded by inert particles. The gas convection starts becoming notable above $Ar = 10^4$ and is equal to particle convection at $Ar = 10^7$. In the important range for fuel conversion $1 < Ar < 10^4$, gas convection heat transfer is small compared to particle convection.

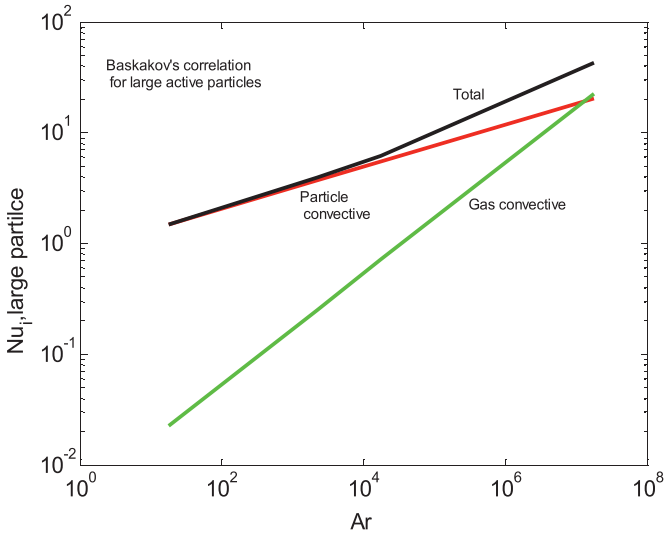

Fig. 2. The components of Eq. (3), heat transfer to a large particle.

The particle convective part in Eq. (3) is very well supported by several investigations for maximum heat transfer, for instance [17] and [21]. Based on a detailed model of gas convective heat transfer, Mazza and Barreto [22] found that their results agreed well with the description of gas convection heat and mass transfer in the region of interest here. Molerus and Schweinzer [23] presented gas convective heat transfer from packed beds, which agrees well within the range of the parameter variation studied for fluidized beds in [1]. The applicability of the mass transfer results in both fixed and fluidized beds was also noted in [4], verifying the previous experience.

Large particles in a bed of fine particles may move from their position and end up in a less representative location than intended, for instance in the bottom region of the bed. Therefore, in experiments large objects are often fixed in the bed. (See further comments on fixed vs freely moving objects below). In all cases considered, it is assumed that, even for small d_i/d_a, no particle segregation occurs in a bed, or if it happens, efforts are made to avoid it or to treat it separately. If the active particles sink to the bottom or rise to the surface, the heat transfer will be affected [18]. Likewise, in some investigations like that of Palchonok and Tamarin [13] it is explicitly stated that, depending on their size and density, particles may float or sink, but such situations were excluded in the evaluation of the data.

The influence of the size of the active particle is seen qualitatively in many results. The best description is found in Prins [24, Chapter II, Fig. 5, and Chapter III, Figs. 3 and 4]. There, the magnitude of the heat or mass transfer coefficients falls gradually as the size of the active particle increases. In fact, the coefficients approach asymptotic values, while the impact of the size of the active particle declines and disappears. This is indirectly supported by Barbosa et al. [25] who claim that the size of d_a has no significance for larger active particles than about 7 mm. (This appears a low limit, but it also depends on the size of the inert particles and property data. The argument was based on the well-known Zabrodsky [17] correlation, which is valid for large active particles in the range where it is not affected by the size of the receiving particle).

The observation on the asymptotic behaviour is confirmed by the striking coincidence between Eq. (3) and the asymptotic heat transfer values (when $d_a \rightarrow$ infinity) in Prins' data, such as shown in Fig. 3. There is a reasonable agreement between Baskakov's data for large fixed active "particles" and the asymptotic values read from Prins' diagrams as the size of the active particle goes to infinity. Some scatter is seen, however, particularly for mass transfer, Fig. 3b. To appreciate the magnitude of the discrepancies, the data read from Prins' diagrams (circles, o) can be compared with what is obtained by Prins' correlation for mass transfer in the case $d_i/d_a = 0$ (crosses, +). The circles and the crosses intend to depict the same thing, and the difference between them is not more than what could be expected from the uncertainty in describing an asymptotic limit. It should be noted that Prins studied the difference between a freely moving and a fixed object in the bed and found that the transfer was always somewhat larger to the fixed object for small bed particles, but it was less for the larger bed particles investigated. For mass transfer Prins [24, Chapter III, Fig. 6] shows an influence of the size of the heat transfer probe used in [26] that seems to contradict the above conclusion on the asymptotic behavior. However, the data concerned measurements on tubes with diameters of $\leq$10 mm. For larger tubes, $\geq$10 mm, no significant influence of tube size was observed in [26], which confirms the above statements on the asymptotic behavior.

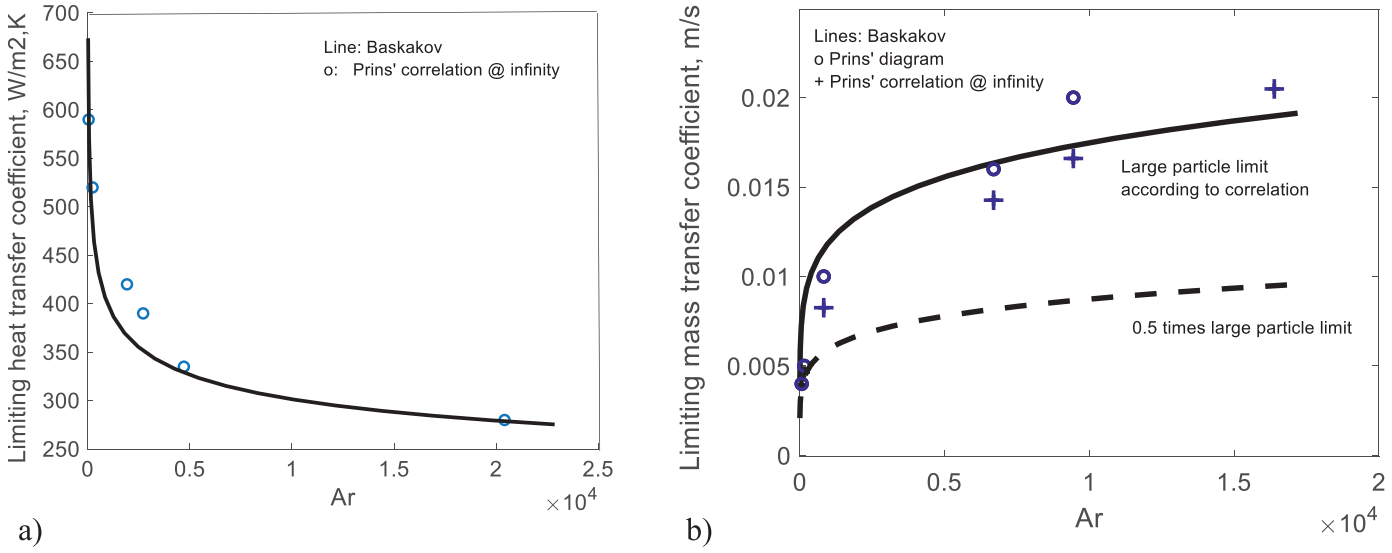

Fig. 3. The asymptotic (a) heat and (b) mass transfer coefficients from Prins' data (symbols) compared with the heat and mass transfer to large particles from Eqs. (3) and (4) (lines).

In conclusion, a moving particle has about the same values of heat transfer coefficient as a fixed large particle. This is shown by Prins' [24] experimental results: only for small bed particles some difference was observed, which, however, was not seen in Fig 3a. In the case of mass transfer, on the other hand, Prins et al. [4] observed that a fixed object has 20-50% higher values than a moving object, and this was partly supported by the above-mentioned experiments by Berg and Baskakov [26]. To illustrate the effect of such a change, the large-particle asymptote is reduced by 50%, as shown by the dashed curve in Fig. 3b.

Prins' observation on the mobility of a particle was supported by Turton et al. [12], who made this experience with fixed and loose wires, submerged in a fluidized bed. In contrast, in [27] the heat transfer was enhanced when an object was free to move. More details are needed to explain these contradictions.

The above discussion concerns two cases: The heat transfer data are in a size range of bed particles where particle convection dominates (Fig. 2). Gas convection contributes only in beds of very large particles. However, in mass transfer, gas convection dominates for all particle sizes.

In conclusion, the representations of the limits, Eqs. (1) to (4), are supported by many independent investigations and appear to be reliable, except for a minor influence, yet to be specified in detail, from the mobility on the large active-particle limit for mass transfer, Eq. (4).

3. Comparisons

3.1. Parameters

In published correlations *Nu* or *Sh* are related to Re_{mf}, Re_{opt} or *Ar*. For a comparison between correlations, they should be translated into the same form, preferably related to *Ar* (d_i). Both Prins [24] and Scala [28] use Re_{mf} in their mass transfer correlations. For heat transfer, the correlations could be related to minimum or optimum fluidization velocity, but *Ar* also expresses these quantities. The Reynolds numbers can be converted into the Archimedes number, because the active particle is supposed to be in the particle phase most of the time subjected to minimum fluidization, or for larger particles, under the condition of maximum heat transfer (at optimum fluidization velocity). The translation between *Re* and *Ar* is achieved by the relationships of Aerov and Todes [29]. The results from these relationships coincide with those of similar expressions [30].

$$\mathrm{Re}_{mf} = Ar/\left(1400 + 5.22Ar^{1/2}\right) \tag{11}$$

$$\mathrm{Re}_{opt} = Ar/\left(18.0 + 5.22Ar^{1/2}\right) \tag{12}$$

To make a comparison possible, the correlations in Table 2, which are not already expressed in Nu_i, are transformed by Eqs. (7) or (8) and as a function of the Archimedes number, according to Eqs. (11) and (12), times a diameter ratio d_i/d_a, which has a power of *n* around 0.2 (partly depending on the definition of Nu related to d_i), expressed as $Nu_i = f(Ar)(d_i/d_a)^n$.

3.2. Heat transfer results

Table 2 and the corresponding Fig. 5 summarize a set of correlations from literature, selected to be the most comprehensive and straight-forward to evaluate.

Shah [31] established and verified a correlation for fixed cylinders and spheres in a fluidized bed. Palchonok and Tamarin [13] studied moving active particles in coarse particle beds. Prins [24] carried out a study on moving particles, covering a wide range of parameters. Tsukada and Horio [32] collected and synthesized all available information at the time, including their own previous work. Barbosa et al. [25] performed a study covering relevant parameter ranges. Scott et al. [15] focused on the low velocity range near minimum fluidization and used freely moving active particles (just like in most other similar studies, the particle was attached to a flexible thermocouple). The particle sizes were rather large in the case of Joulié et al. [33] and Joulié and Rios [34], containing a large collection of data in the form of dimensional and dimensionless correlations. Unfortunately, there is some difficulty in interpretation of the details in the conditions for the correlations in the latter investigations, and it can only be stated that the results coincide grossly with those presented here, with one important difference: the ratio of the densities of active and inert particles was found to be important in contrast to Palchonok and Tamarin [13] who found this influence insignificant as long as the bed was well fluidized. In the other correlations of Table 2 the density ratio is not considered.

The correlations are presented in plotted form for different active particle sizes versus the Archimedes number (the inert bed-

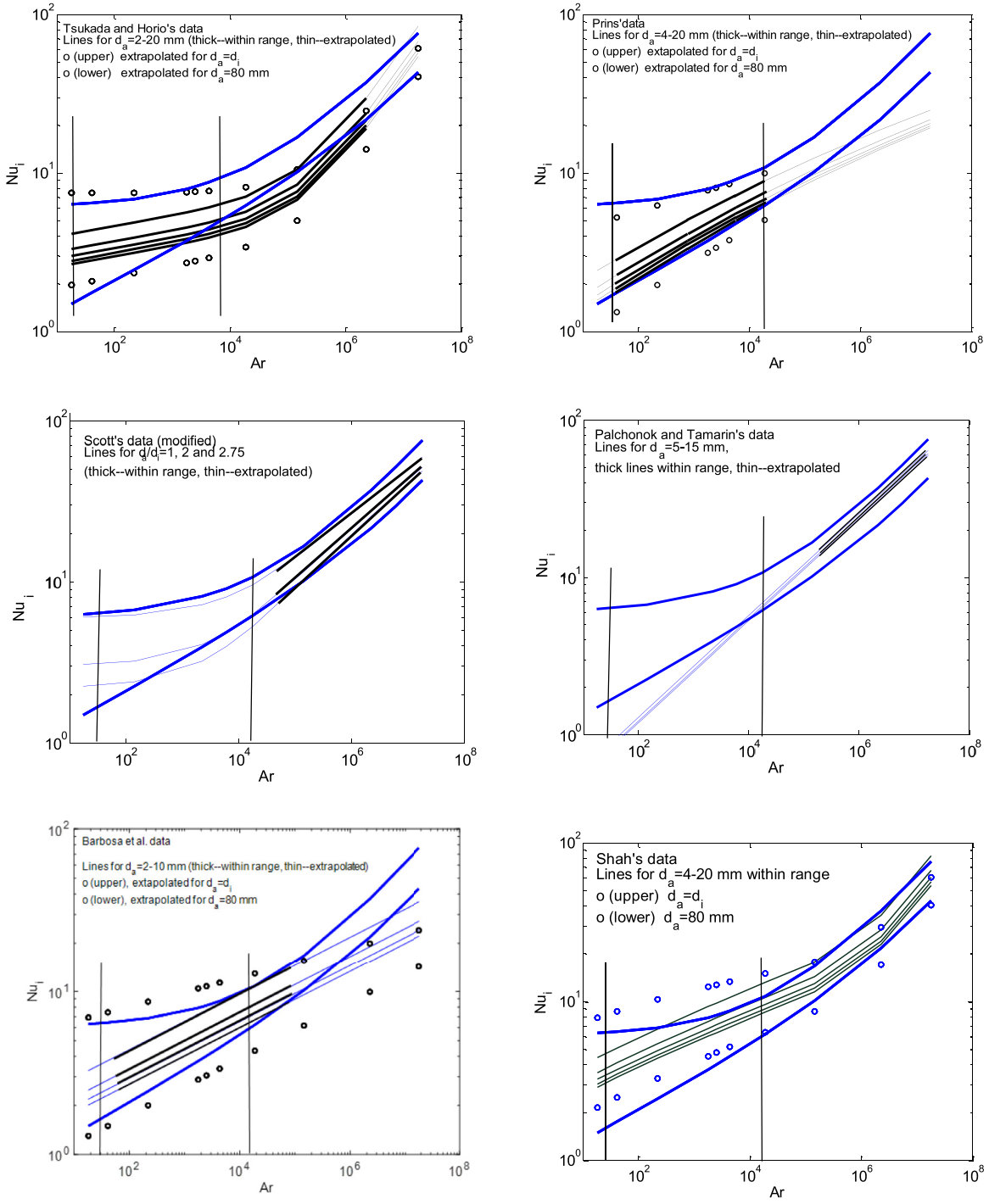

Fig. 4. Summary of the correlations in Table 2, plotted as thin lines within the frame of Eqs. (1) and (3) (thick blue curves) at 600 K. The thick parts of the correlation lines are the parameter ranges where the correlations are supported by measured data. The *Ar* range of primary interest for fuel conversion is marked by vertical lines. (For interpretation of the references to colour in this figure legend, the reader is referred to the web version of this article.)

particle size) in Fig. 4. In general, the data are contained between the limits represented by Eqs. (1) and (3) in a wide span of *Ar*.

Some additional terms in the original publications have been disregarded as they were claimed to have a small impact. In general, the active particles are freely moving in the size range of 2 to 20 mm, whereas Shah's data cover a much wider range of fixed objects (cylinders). The bed particles range from the conditions in beds for fuel conversion, whose particles are often sand-like with sizes between 0.0001 and 0.001 m, and the temperature is between 300 and 1100 K, so the gas density is between $\rho_g = 1.3$ and 0.3 kg/m^3. The inert particles have a solid density of $\rho_i = 2500$ to 2700 kg/m^3 and the dynamic viscosity varies with temperature between $\mu = 1.9 \bullet 10^{-5}$ and $4.5 \bullet 10^{-5}$ kg/m s. This means that *Ar* is between 5 and 5000 in this application at 1100 K. At room temperature the corresponding *Ar* is 100 to 100000. Those limits are indicated in the diagrams. Two of the correlations, [15] and [13], are based on large *Ar*, and they also have a limited range of d_i/d_a. The case of $d_i/d_a = 1$ was particularly treated in Fig. 1, and therefore this limit is also presented as circles in Fig. 4, although in most cases the data are extrapolated from the measured ranges and the

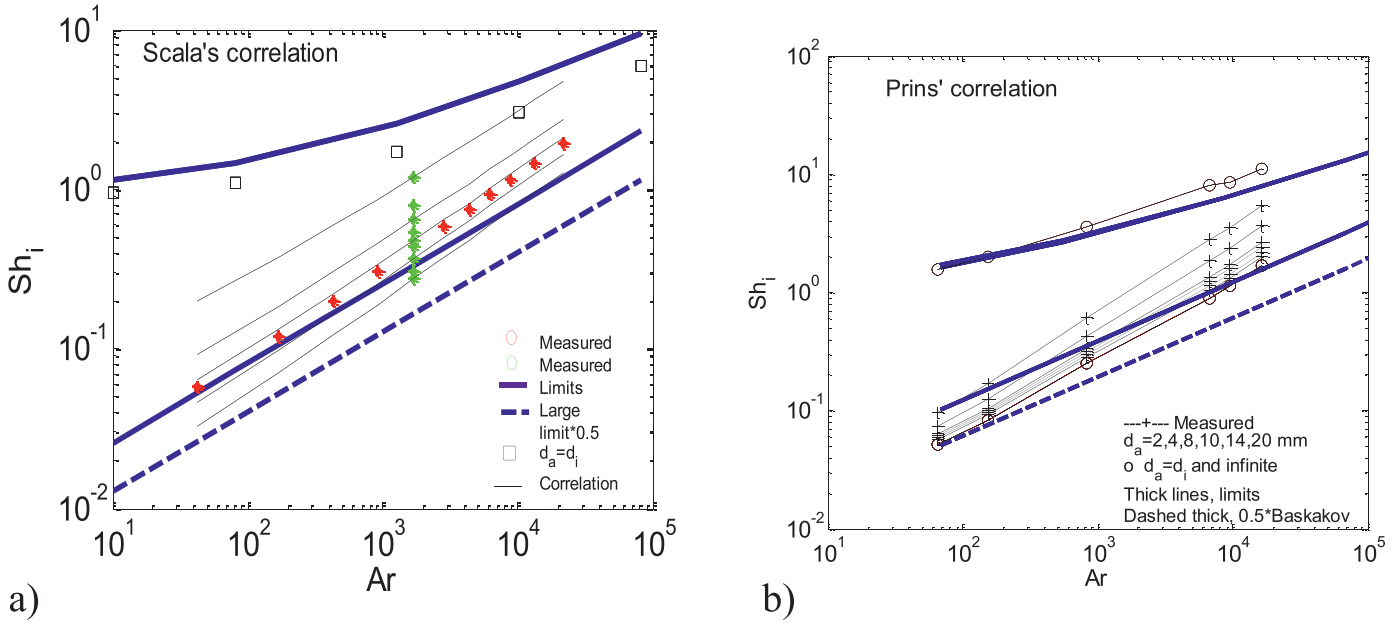

Fig. 5. Results from Scala's [28] (a) and Prins' [4] (b) correlations for mass transfer coefficient shown as $Sh_i=f(d_a,Ar)$. Resulting values for $d_a = d_i$ and for $d_a \rightarrow$large are also shown. Scala: d_a = 1, 2.5, 4, 6.1, 10 mm; T = 723 K, ρ_s = 2500 kg/m^3, Sc = 0.74, ε = 0.44; Prins: T = 338 K, ρ_s = 2750 kg/m^3, Sc = 2.6, ε = 0.40. The thick dashed lines are 50% of the low limit, added for comparison.

agreement is moderate. Likewise extrapolated is the d_a = 80 mm case, illustrating the fact that the correlations are not restricted to a large particle limit but continue to $Nu_i(Sh_i)$=0 for $d_i/d_a \rightarrow 0$. The best behavior in relation to Eqs. (1) and (3) is shown by Prins' correlation if applied in the range of measurements.

Prins used the data of Hsiung and Thodos [14] at $d_i = d_a$ to support his correlation. Therefore, the correlation agrees rather well with Palchonok's correlation, Eq. (1), in this limit. The only deviation from the small particle-size limit, represented by Eq. (1), is that Prins did not include a conduction term, which creates a gap at very low Ar. Scott's correlation [15], on the other hand includes such a term, $2d_i/d_a$, if related to Nu_i. The agreement between Scott's extrapolated correlation and the present data was found to be better if 2 is replaced by 6 to coincide with Palchonok's term, and this is used in Figs. 1 and 4.

There is a qualitative agreement between the various data sets in Fig. 4 and the data are mostly contained between the limits defined above: the $d_a = d_i$ limit and the large active-particle limit. However, the data sets show considerable individual features. They were measured in quite different parameter ranges. The expressions are empirical relationships and cannot really be extrapolated beyond the range of measurements, although some correlations appear to represent data outside of the measured ranges reasonably well.

3.3. Mass transfer correlations

Mass transfer to particles in fluidized beds has been more studied than heat transfer. A recent review summarizing previous work was presented by Scala [28,35], and this background does not have to be repeated here. Focusing on correlations (and avoiding models or semi-empirical developments), it can be concluded that correlations of the Frössling type (the form used for single phase flow) are common also in the fluidized bed application, as seen in Table 3. Early proposals for fluidized beds did not clearly specify the definition of the Reynolds number. La Nauze and Jung [36] pointed out that the active particle was contained in the particle phase, consisting of inert particles, and the relevant velocity experienced by the particle should be $(u/\varepsilon)_{mf}$, although La Nauze and coworkers [37] were uncertain about the choice of velocity u. Later, Hayhurst and Parmar [38] verified this matter and stated that the velocity is related to the minimum fluidization of the inert bed particles, constituting the particle phase (d_i) of a fluidized bed, while Sh and Re are related to the size of the active particle, d_a. Then, with the conduction term according to Avedesian and Davidson [16], the expression got the forms shown in Table 3. This form was also exploited by Scala [28] who carried out well planned and carefully verified experiments. Another important relationship is that of Prins [24] also shown in Table 3, translated from the original formulation into the present terminology, as shown in the Supplementary material.

The results of Table 3 are transformed from the formulations in the table to allow a comparison with Eqs. (2) and (4) in Fig. 5.

Scala (Fig. 5a) carried out his measurements for different active particle sizes at d_i = 0.55 mm (Ar = 2000) and for d_a = 4.6 mm in a range of bed particle sizes of 0.16 <d_i<1.3 mm (40<Ar<20000 @723 K). This gives a cross of measurement points marked in Fig. 5a, supporting his correlation in a rectangular area of validity. Extrapolation outside of this area is possible but does not coincide with Eq. (2), as can be seen from the square symbols representing the $d_a = d_i$ limit, to be discussed below. Extrapolation towards very large active particles becomes unrealistic in this formulation; it tends towards $Sh_i = 0$ when $d_a \rightarrow \infty$.

Prins measured over a wider range (Fig. 5b). Moreover, he complemented his data with the mass transfer coefficients of Hsiung and Thodos [14] allowing him to cover the entire range of active particle sizes down to $d_a = d_i$. In addition, he identified the large active particle limit from where the size of the active particle loses its significance. This is included in his correlation and is depicted by circles in Fig. 5b. Just like in Fig. 3b it is clearly seen that Prins' results, and probably also those of Scala, are below the limiting mass transfer defined by Baskakov's measurements (lower thick solid line in Fig. 5a and b) in the lower Ar region. There is only a possible explanation for this deviation, given by Prins: the mass transfer to a fixed object in a fluidized bed is higher than that to a mobile particle, such as used by Scala and Prins. If this is the case, being 20-50% as Prins et al. [4] mentioned, Baskakov's relationship

could be reduced with the corresponding amount, as illustrated by the dashed line in Fig. 5. However, such a reduction only occurs at small bed particles, as also seen in the linear-scale diagram of Fig. 3b. Furthermore, this phenomenon is only observed in relation to the gas-convective term (mass transfer), which, in the heat transfer case, only plays a role at large bed material (large *Ar*). Accordingly, it is not noticed in the above heat transfer correlations (see Fig. 3a).

3.4. Variation of media properties

The dynamic viscosity and gas density (related to type of gas and temperature), particle size and density, but also other data, such as voidage, may influence the results. However, the relative variation of temperature is similar for the two most important parameters, *Ar* and Re_{mf}. Comparisons were carried out using the data of the respective correlation compared with the Baskakov-Palchonok model.

The property data play a role, and this may impair the agreement between correlations like, for example, those of Scala and Prins, despite the great care taken in the performance of these experiments. Small deviations occur, because of the choice of data *(T, D,* and ε) despite the fact that the correlations are expressed in dimensionless form. Fig. 6 shows a comparison between Scala's and Prins' results. In Fig. 6a Scala's data are used in both cases, and in Fig. 6b Prins' data are used in both cases with input from Table 4. The conclusion is that the property data have an influence. The influence of temperature on *Ar* is also seen in the two diagrams.

The two investigators have established their correlations at slightly different voidages (it should be mentioned that both investigators chose a voidage that was representative to their bed material). The impact of the voidage follows directly from the correlations. Another important deviation is that between Eq. (2) and Scala's correlation extrapolated to $d_a/d_i = 1$ in Fig. 5a. Like the other comparisons, the same property data were used in both correlations. This discrepancy should be judged by comparing differences between the data seen in Fig. 1 and in the original [2] as well as in Scala's and Prins' results, illustrated in Figs. 5 and 6.

4. Development of correlations

It would not be meaningful to try to find average values by combining the various correlations into one. Instead, the strategy employed here is to distribute the active particle sizes between the small ($d_a = d_i$) and the large active particle ($d_a \to \infty$) limits proportionally, as shown by Eqs. (5) and (6) and illustrated in Fig. 7a with iso-d_i/d_a curves for heat and for mass transfer.

The interpolation function $f(d_i/d_a)$ could have various forms, but the scatter of data does not justify elaborate functions, and $f(d_i/d_a) = (d_i/d_a)^n$ with $n \approx 2/3$ results from a rough fit to measurement data. The function should be unity for active and inert particles of equal size (index 1), giving $Nu_i = Nu_1$, and it should be zero when $d_a \to \infty$, yielding $Nu_i = Nu_{i,\infty}$.

Fig. 7b shows d_i/d_a curves for heat transfer, expressed in the form of Nu_i as a function of d_a for two sizes of bed particles d_i, one small (0.1 mm, about $Ar = 20$) and one large (1 mm, about $Ar = 20000$) representing the range of bed materials commonly used in fuel converters. Correlations from Table 2 are included for comparison. The curves start at $d_a = d_i$ and approach the large active particle-limit gradually for each of the two d_i's chosen for the diagram. The curves for the large d_i particles cross the large d_a limit and continue towards low Nu_i. Two striking impressions should be commented upon: 1) The agreement between the curves and the various correlations is not good, as is obvious from the rather scattered results of the correlations shown in Fig. 4; 2) The large active particle limit is usually exceeded when the correlations are extrapolated beyond their range of validity for large d_a, because the term $d_i/d_a \to 0$ as $d_a \to \infty$. This problem is avoided by Eq. 5. The available correlations are intended for the range covered by measurements, but not for data exceeding that range. Often the limits cannot be seen from the correlations themselves. In most cases they are not seen from the presentations of the measured data, as their limits are expressed in ranges of d_a and d_i rather than d_i/d_a.

Curves for mass transfer, made in the same way are presented in Fig. 8 with $n \approx 1$.

The fit to Eq. (6) with $n = 1$ is not perfect for mass transfer either. Fitting is complicated by the disagreement between the measured data sets. Here, the fitting was made with the property values used by Scala [28] (723 K and $Sc = 0.7$). If Prins' [4] values (338 K and $Sc = 2.6$) had been used instead, Prins' curves would have been closer to the present representation. The reduction of the large active particle asymptote by 50% (Fig. 8b) improves the representation, as seen by comparing Fig. 8a and b, but it is not obvious that the complication involved is motivated. The impact of property data is equally important.

Table 3
A few mass transfer correlations.

Source	Mass transfer correlation	Experimental conditions
Scala [28]	$Sh_a = 2.0\varepsilon_{mf} + 0.7(\frac{Re_{mf,a}}{\varepsilon_{mf}})^{0.5} Sc^{0.3}$	Sh_a,Re_a based on d_a $0.1 < d_i < 1.18$ mm $1 < d_a < 10$ mm; 723 K.
Hayhurst and Parmar [38]	"	Sh_a,Re_a based on d_a d_i=0.3; 0.5; 0.6; d_a>3mm; 1000-1200 K.
La Nauze et al. [37]	"	Coke particles 3-15 mm in sand 0.665-0.925 mm, 1000-1200 K.
Prins et al. [4]	$Sh_i = [\frac{1-\varepsilon_{mf}}{\varepsilon_{mf}}]^m [\frac{Re_{mf,i}}{\varepsilon_{mf}}]^{1-m} Sc^{0.33}(0.105 + 1.505(d_i/d_a)^{1.05})$ $m = 0.35 + 0.29(d_i/d_a)^{0.5}$ and $Re_{mf,i} = u_{mf} d_i/\nu$	$0.1 < Re_{mfi} < 20$ $1 < d_a/d_i < 200$ $0.098 < d_i < 0.620$ mm 338 K. Supplementary material

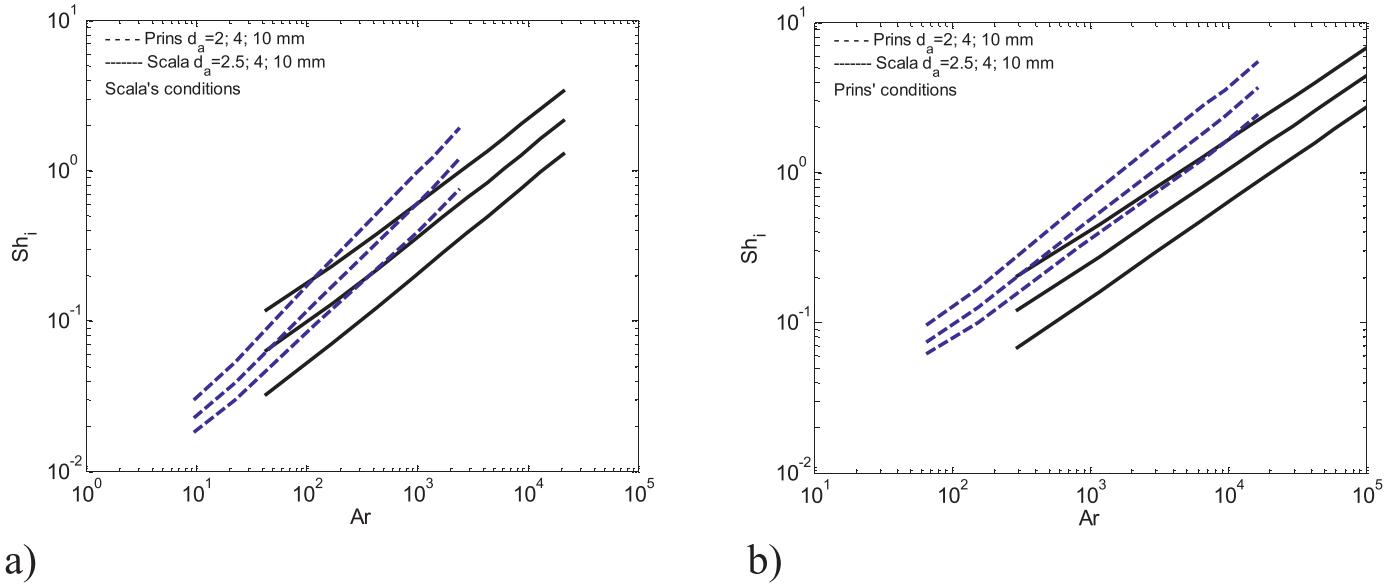

Fig. 6. Comparison between Prins' [4] and Scala's [28] mass transfer data $Sh_i = f(d_a,Ar)$ for two sets of property data used originally by Scala (a) and by Prins (b), see Tables 4 and Fig. 5. Relationships for three active particle sizes are shown in the range of bed particles covered by measurements.

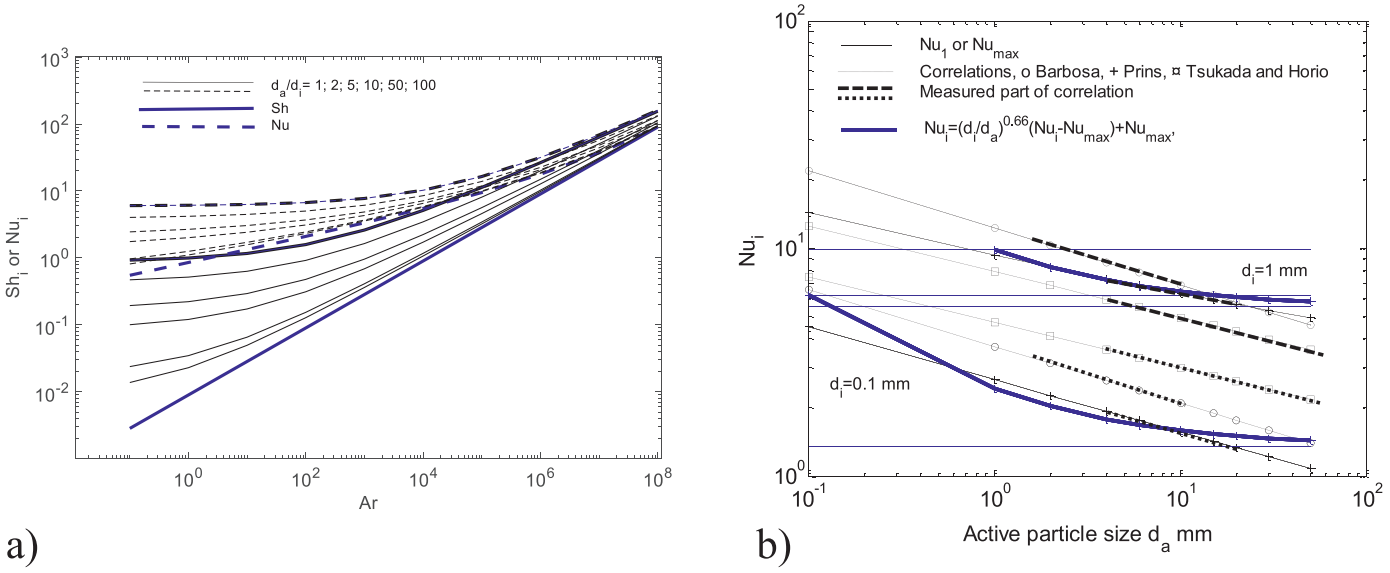

Fig. 7. (a) Nu_i and Sh_i for active particle sizes between the limiting values. (b) Interpolation curves for bed particles (d_i) between 0.1 and 1 mm, plotted vs the diameter of the active particle d_a compared with some correlations. The parts of the correlations covered by measurements are drawn thick. Three data sets are inserted in the diagram for comparison between $d_a = 1$ and 10 for each bed particle size, d_i=0.1 and 1.0 mm.

5. Extension and ranges of validity

5.1. Influence of fluidization velocity

The data treated above are from well-fluidized regions in bubbling fluidized beds, mostly operated at or above the optimum velocity for maximum heat transfer. Even in this situation, a particle exchanging heat or mass may encounter itself in regions with non-representative fluidization conditions: A large particle may sink to a bottom layer (segregation) or it may move in the descending particle streams, meeting a lower gas velocity where the bed movement is less vigorous than in the well-fluidized regions of the vessel, for which the heat and mass transfer correlations are valid.

Another deviation occurs at fluidizing velocities between the minimum and the optimum ones, where the heat transfer is lower than that at the optimum velocity, as shown recently by von Berg et al. [5]. Then, the present results must be completed by modelling. Reference [5] gives an example of such a procedure. The region between minimum and optimum fluidization may be important in laboratory reactors, and in pyrolysers and some gasifiers. Otherwise, in commercial fuel converters the fluidization velocity is chosen relatively high, far from u_{mf}, and then closer to or above u_{opt}, because operational safety requires to compensate for irregular bed material, diluted by ashes or by impurities from fuels. In addition, because of the desire to operate with low pressure-drop distributors, pressure drop and velocity are optimized to avoid local de-fluidization, often avoiding operation at low fluidization velocities close to the minimum one. Another interesting feature in pyrolysers-gasifiers, operated at low velocity, is the opposite segregation to that mentioned above: light, degasified char particles ascend to the surface of the bed where they float in large groups, affecting mass transfer, Qin et al. [39]. A similar investigation for

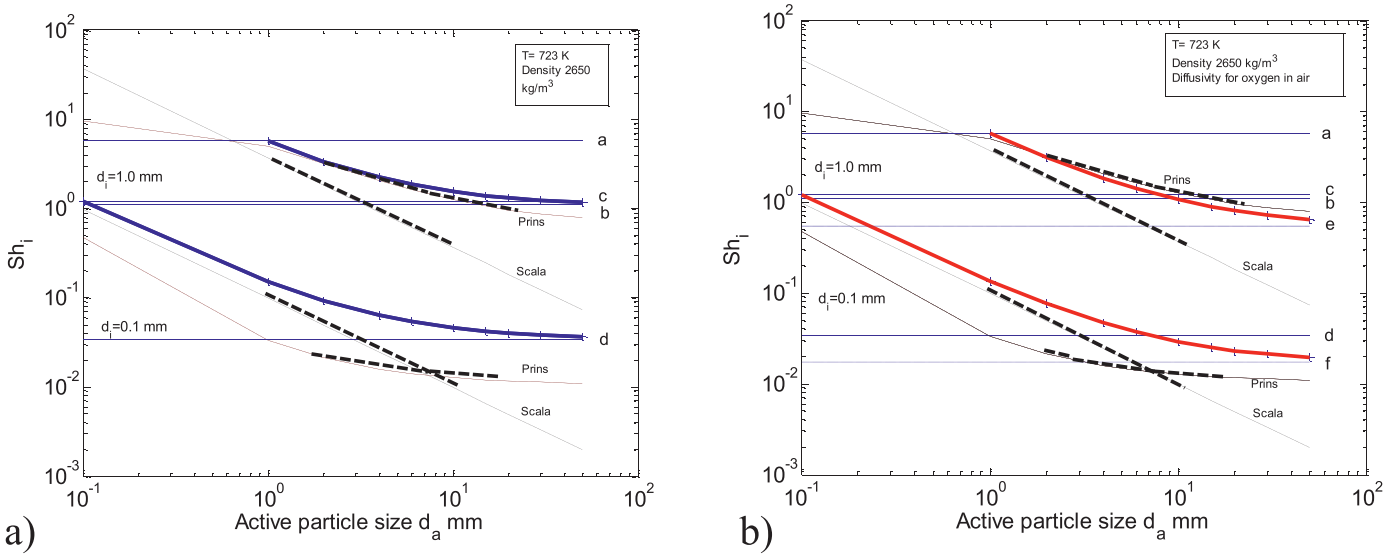

Fig. 8. a. Interpolation curves for mass transfer for 0.1 and 1 mm bed particles (d_i) plotted vs the diameter of the active particle d_a, compared with some correlations. Fig. 8b, the same data as in Fig. 8a but the large-particle limit is lowered by 50%. The thick dashed part of Scala's and Prins' curves represent the measured ranges. The horizontal lines are: (a) Eq. (2) $Sh_{small,0.1mm}$; (b) Eq. (4) $Sh_{large,0.1mm}$; (c) Eq. (2) $Sh_{small,1mm}$; (d) Eq. (4) $Sh_{large,1mm}$; (e) Eq. (4) $Sh_{large,0.1mm}$*0.5; (f) Eq. (4) $Sh_{large,1mm}$*0.5.

heat transfer was not carried out, but heat transfer, in contrast to mass transfer, may be affected by particle convection.

In general, unlike heat transfer, mass transfer depends less on the movement of the bed, and the mass-transfer correlations are not affected as much as the ones for heat transfer.

5.2. Application of heat and mass transfer to active particles in circulating fluidized beds

The conditions in a circulating fluidized bed (CFB) boiler differ from those in laboratory risers: temperature 1100-1200 K, particle size and density 100-300 µm and 1600-2600 kg/m^3, particle circulation rate 10-20 kg/m^2,s, cross-section size 10-20 m, and height 30-50 m.

Circulating fluidized bed is an important field of application where the above relationships are not readily valid. A CFB riser for fuel conversion can be divided into three regions, identified by pressure drop and height (examples are given in brackets): a low bottom bed, whose properties remind of a violently bubbling bed (4000 Pa, 0.5 m), a splash or transition zone (1000 Pa, 2 m) consisting of particles thrown up from the bottom bed, subsequently falling back, except a small quantity of bed particles and fuel that is carried up by the gas and found in the upper part of the riser, forming a particle-lean transport zone (7000 Pa, 40 m). The particle density of $(1-\varepsilon) = \Delta P/(Hg\rho_s)$ with ΔP pressure drop (Pa), g = 9.81 gravity (m/s^2), H m height, and ρ_s = 2600 kg/m^3 bed-particle density, yield with the data mentioned average particle concentrations (1-ε) of 0.30, 0.02, 0.007 for the three zones, if we assume the total pressure drop to be 12000 Pa over the height of 43 m of a 300 MW$_e$ boiler. The active particles are below a few percent of the total particle inventory. The larger of these particles tend to remain in the bottom bed, while the finer active particles and the inert bed material are carried upwards in the riser.

A general form, now related to d_a, of the gas convective and conductive heat and mass transfer, is expressed by the relationships, Eqs. (1) and (2), where the Ar terms have been replaced by the Re terms because they give more freedom in handling the velocity of the particle phase through u/ε

$$Nu_a = \frac{2}{(1-(1-\varepsilon)^{1/3})} + 0.69\mathrm{Re}_{a,s}^{0.5}\mathrm{Pr}^{0.33}$$
$$Sh_a = 2\varepsilon + 0.69\mathrm{Re}_{a,s}^{0.5}Sc^{0.33} \quad (13)$$

The particle convective heat transfer may also be important, at least in the bottom bed, as will be shown below.

The Reynolds number contains the active particle size d_a and the superficial slip velocity u_s, expressed as the velocity felt by the particle, u_s/ε. The voidage ε is that in the vicinity of the particle. In the particle phase of a bubbling bed this term is u_{mf}/ε_{mf}. The relationships are used for flows with low particle concentration ($\varepsilon \to 1$) where their validity is supported by the form for single phase flow. They, at least the mass transfer form, are also valid in the dense phase of a bubbling fluidized bed (Fig. 5), and it can be inferred that they can be applied in intermediate cases between dense and dilute suspensions. In case of large active particles, the heat transfer correlation of Eq (13a) should be completed with a term for particle convection.

In the transport zone, the solids concentration is higher than the limiting value for the formation of clusters, defined by Madsen [40], being (1-ε) = 0.0003. However, Madsen did not specify the particle size. As seen from Bi and Fan [41] the difference between the free fall velocity of a single particle and the transport velocity, which is illustrates the potential influence of cluster flow, grows smaller with the increased size and density of the particles, where everything else is equal. With larger and heavier particles, the impact of clusters becomes less significant. Consequently, Group B particles are less prone to form clusters in a combustor compared with Group A particles in a CFB cracking unit, but nevertheless, clusters could be present in the core of the transport zone of a combustor, and, particularly, in the in its wall layer. Whether clusters play a role or not also depends on the particle concentration as can be judged from a result presented by Nikolopoulos et al. [42], showing a homogeneity index, the ratio of the calculated drag of a homogeneous suspension and that of a clustering one. When the flow properties are in a homogeneous region, clusters play an insignificant role. The transport zone, characterized as above, is quite dilute and mostly belongs to the homogeneous zone, while the transition zone, having a higher particle concentration, is, not surprising, in the heterogeneous zone. Then, Eqs. (13) can be used in the transport zone with $u_s = u_t$, the terminal velocity of a single particle, with $\varepsilon \approx 1$.

The situation in the splash (transition) zone and in the wall-layers is more complicated. In the wall-layers active particles may be included in descending clusters. It is not known which velocity

Table 2
Heat transfer correlations expressed in Nu_i.

Reference	Heat transfer correlation	d_i mm	Ar @ 300 K	d_a mm	d_a/d_i	Experimental conditions
Shah [31]	$Ar < 40000$ $Nu_i = 9.4Re_{opt}^{\ 0.158}(d_i/d_a)^{0.195}(c_{pi}/c_{pg})^{0.18}$ $Ar > 40000$ $Nu_i = 0.574Re_{opt}^{\ 0.695}(d_i/d_a)^{0.195}$	0.104-15	100-3•10^8	0.13-220	1-2000	Fixed spheres and cylinders, 300-1200 K
Palchonok & Tamarin [13]	$Nu_i = 0.41Ar^{0.3}(d_i/d_a)^{0.2}(\rho_a/\rho_i)^{0.07}$	0.62-6.3	1.55•10^5-2.2•10^7	5.2-15	0.8 to 14	Density dep. disregarded. Temperature was not given.
Prins [24]	$Nu_{i,Prins} = 3.539 f_T Ar^m (d_i/d_a)^{0.257}$ $m = 0.105(d_a/d_i)^{0.082}$ $f_T = 0.844 + 0.0756(T_i/273)$	0.131-1.07	200-110000	4-20	3-200	Correction factor f_T for up to 1200 K
Tsukada & Horio [32]	$Nu_{i,Horio} \approx (7.5 + 0.1\,Pr\,Re_{mf})(\frac{d_i}{d_a})^{0.2}$	0.08-3	46-2.5•10^6	4-60	2-300	Supplementary material 293-1320 K
Barbosa et al. [25]	$Nu_i = 5.33Ar^{0.09}(d_i/d_a)^{0.25}$	0.11-0.92	120-66000	1.5-9.4	10-40	400−1200 K
Scott et al. [15] (modified).	$Nu_i = 6d_i/d_a + Re_{mf}^{\ 0.6}(d_i/d_a)^{0.14}$	0.78-9	45000-68•10^6	2-6	0.2-3	Supplementary material. 2 has been changed to 6.<573 K

Table 4
Property data and parameters used by Prins and Scala.

Quantity	Scala	Prins
Temperature, K	723	338
Bed particle density, kg/m^3	2500	2750
Voidage, -	0.44	0.40
Diffusivity, m^2/s	9.4•10^{-10}T$^{1.75}$	2.8•10^{-10}T$^{1.75}$
Sc, -	0.7	2.6

they will experience relative to the falling film, but these particles are not critical for fuel conversion as their temperature falls, at least in a boiler with heat exchanging walls. In the splash zone, particles are ejected by bursting voids, carried away by the high through-flow of gas. At the top of the splash zone, the particles decelerate and most of them fall back to the bottom bed again in a clustering flow, while the finer particles are entrained by the gas into the transport zone. Eq. (13) can be used, but a refined computational analysis is required for an accurate determination of the slip velocity and local bed density. If such computations are not carried out, the average suspension density based on pressure drop can be estimated, while the slip velocity is difficult even to guess. In the absence of anything else, the terminal velocity can be used.

The bottom bed reminds of a bubbling bed composed of a particle phase and bubbles, although much more irregular than a normal bubbling bed of Group B particles. A wide CFB bed will not turn into slugging and turbulent fluidization [43] and the bubbling character is maintained as long as there is bed material left in the bed that has not been distributed along the riser height. The bubbles are irregular voids and the through-flow of gas is considerable, allowing a particle phase to exist, less exposed to a very high velocity and expanding less than a bed of Group A particles [43, Fig 3]. A rough estimate of average bed voidage can be made for a bed composed of a high-velocity void-phase δ and a low-velocity particle phase with a voidage $\varepsilon_e \geq \varepsilon_{mf}$, that is, $\varepsilon_{bed} = \delta + (1-\delta)\varepsilon_e$. Little qualitative information is available from the bottom bed, but rough estimates can be based on the figure referred to in [43], yielding $\varepsilon_{bed,opt} \approx 0.6$ at optimum heat transfer and $\varepsilon_{bed} \approx 0.7$ at higher velocity. Werther and Wein [44] measured the density of the particle phase from where a value, extrapolated to typical conditions, would be $\varepsilon_e \approx 0.58$. This yields $\delta \approx 0.3$ but this number is quite uncertain. Since the gas velocity through the particle phase has to be low (otherwise it would not exist), the velocity through the void phase is high, 10 to 15 m/s. the voids are not free from particles and the entrainment by the void phase creates the splash zone. In this part of the riser, particle convection may contribute to heat transfer, at least to large active particles, and Eq (13a) must be completed by a particle convection component. Because of the similarity of the fluidization features of the bottom bed and a bubbling bed, a slightly modified version of Palchonok's model can be tried, Eqs. (1)–(6). With the uncertainty illustrated in Fig. 5, Eqs. (1 and 2) can be tentatively replaced by Eq. (13) for the case $d_a = d_i$. The particle convection at optimum velocity (Eq. 3) is valid also at higher velocities in conventional beds, but in the CFB bottom bed the velocity is even higher, and the bed is more disperse, as pointed out above. The first term on the right-hand side of Eq. (3) could be compensated for this expansion by multiplication with $(1-\varepsilon_{bed})/(1-\varepsilon_{bed,opt})$ where ε_{bed}, and $\varepsilon_{bed,opt}$ (the actual voidage and that during optimum conditions) are estimated.

Quite clearly, heat and mass transfer to active particles in CFB are not yet well known. It seems from present publications that most interest goes in the direction of catalytic reactors where the conditions are slightly different from those of converters of solid fuels, such as boilers. Notably, there are differences in bed material sizes, pressure drops, circulation rates etc. and particularly in the topic of the present account, in the interaction of active and inert

particles. In catalytic beds, all particles are active (if dilution is not applied), while in converters of solid fuels, the quantity of active particles is less than a few percent of the total amount of particles.

6. Conclusion

In contrast to heat and mass transfer to all particles in a fluidized bed, here a formulation for transfer to active particles in a fluidized bed is analysed, originally proposed by Baskakov and further elaborated by Palchonok. The formulation estimates the distribution of the heat or mass transfer between two limits, depending on the size of the inert particles in relation to the active particles by an empirical function $f(d_i/d_a) = (d_i/d_a)^n$, where $n = 2/3$ for heat transfer and $n = 1$ for mass transfer. The two limits are given by correlations determined by fits to data for small active particles, when $d_i = d_a$, and for a limit approached asymptotically while the active particles grow large, $d_a \rightarrow \infty$, and the size loses its significance. Both limits are supported by measurement data, but there are uncertainties as seen when comparing alternative correlations, notably those of Scala, employing a Frössling type of correlation for mass transfer, and Prins who developed correlations both for heat and mass transfer. Most of the comprehensive sets of measurement data found in literature and their corresponding correlations fit with minor exceptions within the above-mentioned limits, but the detailed mutual agreement between the various correlations is poor, and it is not meaningful to try to find some average value, generalizing all correlations. Moreover, the ranges of measurements are restricted and do not well coincide in the results from different research activities. In most cases, the *Nu* or *Sh* numbers are functions of *Re* or *Ar* (which are related, because Re_{mf} or Re_{opt} are related to the particle phase and its properties), *Pr (Sc)*, and a size ratio $(d_i/d_a)^n$. It is noted that the published correlations selected for comparison do not reach the limits for small and large particles, and the limits defined in the present model are wider than most of the measured ranges in other research results. The correlations quoted could not be safely extrapolated beyond the region covered by measurement data, while the Baskakov-Palchonok correlation covers a wide range of data, including both heat and mass transfer.

It has been shown how correlations can be applied also in CFB solid fuel converters. In this case the critical parameters are the slip velocity in *Re* and the local voidage. These parameters are not well known in all zones of a CFB riser, and with the present knowledge assumptions should made.

Declaration of Competing Interest

There are no conflicts of interest.

Acknowledgement

This work was partly funded by the grant 13145-7 from the Swedish Energy Agency regarding conversion in fluidized bed.

Supplementary materials

Supplementary material associated with this article can be found, in the online version, at doi:10.1016/j.ijheatmasstransfer.2020.120860.

References

[1] A.P. Baskakov, B.V. Berg, O.K. Vitt, N.F. Filippovsky, V.A. Kirakosyan, J.M. Goldobin, V.K. Maskaev, Heat transfer to objects immersed in fluidized beds, Powder Technol. 8 (1973) 273–282.
[2] G.I. Palchonok, A.F. Dolidovich, S. Andersson, B. Leckner, Calculation of true heat and mass transfer coefficients between particles and a fluidized bed, Fluidization VII, Eng. Found. (1992) 913–920.
[3] G.I. Palchonok, Heat and mass transfer to a single particle in fluidized bed, Chalmers University of Technology, Sweden, 1998 PhD Thesis.
[4] W. Prins, T.P. Casteleijn, W. Draijer, W.P.M. van Swaaij, Mass transfer from a freely moving single phase of a gas fluidized bed of inert particles, Chem. Eng. Sci. 40 (1985) 481–497.
[5] L. von Berg, A. Soria-Verdugo, C. Hochenauer, R. Scharler, A. Anca-Couce, Evaluation of heat transfer models at various fluidization velocities for biomass pyrolysis conducted in a bubbling fluidized bed, Int. J. Heat Mass Trans. 180 (2020) 120175.
[6] A. Gómez-Barea, B. Leckner, Modeling of biomass gasification in fluidized bed, Prog. Energy Combust. Sci. 36 (2010) 444–509, doi:10.1016/j.pecs.2009.12.002.
[7] F. Di Natale, R. Nigro, F. Scala, Heat and mass transfer in fluidized bed combustion and gasification systems, in: Chapter 5, Woodhead Publishing Series in Energy, 2013, pp. 177–253.
[8] D.J. Gunn, Transfer of heat or mass to particles in fixed and fluidised beds, Int. J. Heat Mass Transf. 21 (1978) 467–476.
[9] N. Frössling, The evaporation of falling drops [in German], Gerlands Beitr. Geophys. 52 (1938) 170–216.
[10] W.E. Ranz, W.R. Marshall Jr., Evaporation from drops, Chem. Eng. Progr. 48 (1952) 173–180 (part I) 141-146 and (part II).
[11] A.P. Baskakov, N.F. Filippovskii, V.A. Munts, A.A. Ashikhmin, Temperature of particles heated in a fluidized bed of inert material, J. Eng. Phys. 52 (1987) 574–578.
[12] R. Turton, M. Colakyan, O. Levenspiel, Heat transfer from fluidized beds to immersed fine wires, Powder Technol. 53 (1987) 195–203.
[13] G.I. Palchonok, A.I. Tamarin, Study of heat exchange between a model particle and a fluidized bed (Translated), J. Eng. Phys. 45 (1983) 1017–1022.
[14] T.H. Hsiung, G. Thodos, Mass transfer in gas-fluidized beds: measurements of actual driving forces, Chem. Eng. Sci. 32 (1977) 581–592.
[15] S.A. Scott, J.F. Davidson, J.S. Dennis, A.N. Hayhurst, Heat transfer to a single sphere immersed in beds of particles supplied by gas at rates above and below minimum fluidization, Ind. Eng. Chem. Res. 43 (2004) 5632-564.
[16] M.M. Avedesian, J.F. Davidson, Combustion of carbon particles in a fluidized bed, Trans. Inst. Chem. Eng. 51 (1973) 121–131.
[17] S.S. Zabrodsky, N.V. Antonishin, A.L Parnas, On fluidized bed to surface heat transfer, Can. J. Chem. Eng. 54 (1976) 52–58.
[18] S. Cobbinah, C. Laguérrie, H. Gibert, Simultaneous heat and mass transfer between a fluidized bed of fine particles and immersed course porous particles, Int. J. Heat Mass Transf. 30 (1987) 395–400.
[19] G.I. Palchonok, Heat and mass transfer of moving particles in a fluidized bed of highly dispersed material, in: R.I. Soloukhin (Ed.), Heat and Mass Transfer; Theory and Practical Applications (In Russian), BSSR, 1983, pp. 41–50. R.I, ITMO, Akademii Nauk.
[20] A.P. Baskakov, V.M. Suprun, Determining the convective component of the heat-transfer coefficient to gas in a fluidized bed, Khim. Neft. Mashinostr. (3) (1971) 20–21.
[21] N.N. Varygin, I.G. Martyushin, Calculation of the heat transfer surface in fluidized bed equipment, Khimicheskoe Mashinostroenie 5 (1959) 6–9 (in Russian.
[22] G.D. Mazza, G.F. Barreto, The gas contribution to heat transfer between fluidized beds of large particles and immersed surfaces, Int. J. Heat Mass Transf. 31 (1988) 603–614.
[23] O. Molerus, J. Schweinzer, J.R. Grace L.W. Shemit, M. Bergougnou (Eds.), Banff, 1989.
[24] W. Prins, Fluidized bed combustion of a single carbon particle, Thesis, Twente Univ., 1987.
[25] A.L. Barbosa, D. Steinmetz, H. Angelino, Engineering Foundation, 1995, pp. 177–186.
[26] B.V. Berg, A.P. Baskakov, Experimental investigation of heat transfer between a fluidized bed and a cylindrical surface, J. Eng. Phys. 11 (1966) 42–47.
[27] G. Rios, H. Gibert, Engineering Foundation, 1983, pp. 363–370.
[28] F. Scala, Mass transfer around freely moving active particles in the dense phase of a gas fluidized bed of inert particles, Chem. Eng. Sci. 62 (2007) 4159–4176.
[29] M.E. Aerov, O.M. Todes, Hydraulic and Thermal Fundamentals on the Operation of Apparatus with Static and Fluidized Particle Bed (In Russian), Chimia, Leningrad, 1968.
[30] D. Kunii, O. Levenspiel, Fluidization Engineering, Butterworth-Heinemann, 1991.
[31] M. Shah, Generalized prediction of maximum heat transfer to single cylinders and spheres in gas-fluidized bed, Heat Transf. Eng. 4 (3-4) (1983) 107–122.
[32] M. Tsukada, M. Horio, Maximum heat transfer coefficient for an immersed body in a bubbling fluidized bed, Ind. Eng. Chem. Res. 31 (1992) 1147–1156.
[33] R. Joulié, M. Barkat, G.M. Rios, Effect of particle density on heat and mass transfer during fluidized bed sublimation, Powder Technol. 90 (1997) 79–88.
[34] R. Joulié, G.M. Rios, Theoretical analysis of heat and mass transfer phenomena during fluidized bed sublimation, Drying Technol. 11 (1993) 157–182.
[35] F. Scala, Mass transfer around active particles in fluidized beds, in: M. El-Amin (Ed.), Mass Transfer in Multiphase Systems and Its Applications, 2011 ISBN: 978-953-307-215-9.
[36] R.D. La Nauze, K. Jung, in: 19th Symp. (Int.) on Combustion, The Combustion Institute, Pittsburgh, 1982, pp. 1087–1092.
[37] R.D. La Nauze, K. Jung, J. Kastl, Mass transfer to large particle particles in fluidized beds of smaller particles, Chem. Eng. Sci. 39 (1984) 1623–1633.
[38] A. Hayhurst, M.S. Parmar, Measurement of the mass transfer coefficient and Sherwood number for carbon spheres burning in a bubbling fluidized bed, Comb. Flame 130 (2002) 361–375.

[39] K. Qin, H. Thunman, B. Leckner, Mass transfer under segregation conditions in fluidized beds, Fuel 195 (2017) 105–112.
[40] J.M. Madsen, Mechanisms of choking and entrainment, Powder Technol. 32 (1982) 21–33.
[41] H.T. Bi, L.S. Fan, Existence of turbulent regime in gas–solid fluidization, AIChE J. 38 (1992) 297–301.
[42] A. Nikolopoulos, C. Samlis, M. Zeneli, N. Nikolopoulos, S. Karellas, P. Grammelis, Introducing an artificial neural network energy minimization multi-scale drag scheme for fluidized particles, Chem. Eng. Sci. 229 (2021) 116013.
[43] B. Leckner, Regimes of large-scale fluidized beds for solid fuel conversion, Powder Technol. 308 (2017) 362–367.
[44] J. Werther, J. Wein, Expansion behavior of gas fluidized bed in the turbulent regime, A.I.Ch.E. Symp. Ser. 90 (301) (1994) 31–44.